Available online at www.sciencedirect.com
ScienceDirect
Polyhedron 26 (2007) 2413–2419
POLYHEDRON
www.elsevier.com/locate/poly

The utility of the single-molecule magnet Fe_8 as a magnetic resonance imaging contrast agent over a broad range of concentration

Brant Cage [a,*], Stephen E. Russek [a], Richard Shoemaker [b], Alex J. Barker [c], Conrad Stoldt [c], Vasanth Ramachandaran [d], Naresh S. Dalal [d,1,2]

[a] National Institute of Standards and Technology, Electromagnetics Division, 325 Broadway, ms 818.03, Boulder, CO 80305, United States
[b] Department of Chemistry and Biochemistry, University of Colorado, Boulder, CO 80390, United States
[c] Department of Mechanical Engineering, University of Colorado, Boulder, CO 80309, United States
[d] Department of Chemistry and Biochemistry, Florida State University, Tallahassee, FL 32306, United States

Received 24 August 2006; accepted 10 December 2006
Available online 14 December 2006

Abstract

Recent reports have compared $Fe_{8(aq)}$ versus Magnevist with seemingly conflicting conclusions: one claims a much greater efficiency of Fe_8 for magnetic resonance imaging contrast, and the other claims a much lower efficiency. Our study shows that at concentrations below 1.5 mM $Fe_{8(aq)}$ had a T_1 relaxivity, r_1, of 5.4 s^{-1} mM^{-1} which is comparable to Magnevist. Above 1.5 mM $Fe_{8(aq)}$ had an r_1 of 1.1 s^{-1} mM^{-1}, significantly lower than Magnevist. These results agree with the previous literature over the concentrations they examined. The results for the T_2 relaxivity, r_2, were similar. Here, we show that the concentration dependence of the relaxivity accounts for these discrepancies. Further, the relaxivity data are correlated with frequency-dependent maxima in χ''_{ac} of frozen solutions of Fe_8 dissolved in deionized water over the temperature range of 1.8–4 K and the frequency range of 200–1400 Hz. The magnetic properties of the single-molecule magnet Fe_8 in room temperature and frozen aqueous solution were found to be highly non-linear when examined over a wide concentration range.
© 2007 Elsevier Ltd. All rights reserved.

Keywords: Fe_8; MRI contrast agent; SMM; ac susceptibility; NMR; Relaxivity

1. Introduction

The design and testing of magnetic resonance imaging (MRI) contrast agents is important for medical diagnostics. MRI contrast agents function by changing the nuclear resonant frequency, the longitudinal energy relaxation time T_1, and the transverse dephasing time T_2, of nearby aqueous hydrogen nuclei in biological systems. These changes allow the medical community to selectively enhance the contrast of structures of interest such as tumors, the vasculatory system, and lesions. The most common MRI contrast agents in current use are the gadolinium chelates and the superparamagnetic iron oxides (SPIO), each of which have their advantages in terms of contrast applications [1]. Recently, there has been interest in the literature for using materials that bridge the gap between the constrained chemical and magnetic structure of the gadolinium chelates with the superparamagnetism of the SPIOs [2–4]. One class of materials that may meet this need are the single-molecule magnets (SMM). These nanometer-scale magnetic structures possess large adjustable moments with anisotropy energies that allow remnant moment and controllable magnetic fluctuations. Among these, the SMM $[Fe_8O_2(OH)_{12}$(1,4,7-triazacyclononane)$_6]Br_8 \cdot 9H_2O$, henceforth Fe_8, has

* Corresponding author. Tel.: +1 303 497 4224; fax: +1 303 497 7364.
E-mail address: bcage@boulder.nist.gov (B. Cage).
[1] Contribution of the National Institute of Standards and Technology; not subject to US copyright.
[2] Certain commercial contrast agents are identified to specify the experimental study adequately. This does not imply endorsement by NIST or that the contrast agents are the best available for the purpose.

0277-5387/$ - see front matter © 2007 Elsevier Ltd. All rights reserved.
doi:10.1016/j.poly.2006.12.009

dimensions <2 nm and is superparamagnetic [5]. Here, "superparamagnetic" denotes a magnetic system that has an anisotropy energy (or a zero field splitting) resulting in a fixed moment at low temperatures, and a fluctuating moment at temperatures above the corresponding anisotropy energy. Fe_8 is one of the best chemically and magnetically characterized materials. Much of the focus of the research on SMMs has been geared towards its fundamental chemical [6], EPR spectroscopic [7–12], and magnetic properties [13–15]. Potential solid-state applications of SMMs are use in high density magnetic memory, quantum computing [16], and spintronics devices such as high-frequency spin-based oscillators and signal processors [17].

Three recent studies have indicated potential applications of these materials dissolved in aqueous solution as versatile MRI contrast agents [2–4]. Rodriguez et al. published a comprehensive work comparing MRI phantoms at 64 MHz (1.5 T), and nuclear magnetic resonance (NMR) results at 400 MHz (9.4 T) for $Fe_{8(aq)}$ with Gd-DTPA (DTPA = diethylenetriamine-pentacetic acid) obtained as the commercial preparation Magnevist [2]. They found that the relaxivities of $Fe_{8(aq)}$ were about equal to that of Magnevist at 64 MHz and possibly superior at higher resonance frequencies [2]. They also examined the cytotoxicity of Fe_8 and found a lethal concentration for 50% mortality, LC_{50}, of ~1 mM [2]. Isaacman et al. also compared Fe_8 versus Magnevist using NMR relaxivity at 400 MHz [3]. They found, however, that $Fe_{8(aq)}$ was much less efficient than Magnevist for MRI contrast applications [3]. In a study of tailored iron-based imaging agents using MRI phantoms at 64 MHz, Barker et al. compared de-ionized (DI) water and DI water containing the dissolved Fe_8, and found that $Fe_{8(aq)}$ had potential as a contrast agent for both the T_1 and T_2 weighted contrast experiments [4]. Barker et al., however, did not provide any quantitative comparisons with Magnevist [4]. To resolve the conflict we undertook the current study to determine the relative merits of $Fe_{8(aq)}$ and Magnevist as a function of concentration.

The spin arrangement of the SMM Fe_8 at low temperatures can be thought of as a spin $S = 10$ particle where six $S = 5/2$ Fe^{3+} are aligned antiparallel to two $S = 5/2$ Fe^{3+} [5]. In general, this compound is modeled using a double-well potential with each well minimum corresponding to the preferred moment orientations. The depth of this well, $\Delta E/k$, (where k is the Boltzmann constant and ΔE is the anisotropy energy or barrier to reorientation) is about 24 K [18,19]. This results in Arrhenius-like thermally activated slow relaxation of the magnetization such that the magnetization fluctuation time is, $\tau = \tau_0 e^{\Delta E/kT}$, where τ_0 is the characteristic oscillation time in the energy well and T is the temperature. At temperatures of less than 1 K the dc magnetization of Fe_8 becomes constant relative to the typical measurement time of 100 s [20]; some SMMs have been shown to take months to relax [5]. This phase will be referred to as the blocked phase. Above 1 K each Fe_8 molecule fluctuates rapidly relative to this measurement time scale and the dc magnetization begins to decrease with increasing temperature, similar to a paramagnet, and due to the large moment per molecule is referred to as the superparamagnetic phase. This temperature dependent fluctuation time will lead to a frequency-dependent susceptibility. At room temperature the magnetic structure is less well known and will be more complex than an $S = 10$ macrospin particle.

The attractive qualities of Fe_8 for MRI contrast are aqueous solubility, possible ligand modification for bioconjugation, the large moment per molecule; and, unlike larger iron particles derived from solvo-thermal synthesis and top–down deposition techniques, these molecules are homogenous, identical units. The unknown quantities investigated here are the relaxivity over a range of concentrations spanning both previous studies using NMR and MRI techniques at 300 and 64 MHz, respectively, and the solution phase chemical identity using a novel ac susceptibility (χ_{ac}) study as a function of concentration. We then correlate the results from χ_{ac} with the relaxivity data to demonstrate why, in fact, both previous studies are correct at the relevant range of concentration.

2. Experimental

2.1. Synthesis

Fe_8 was synthesized in single crystal form using the original method of Weighardt [6] and summarized in earlier reports [7,9,21].

2.2. Ac susceptibility

The χ_{ac} data were obtained at zero applied dc magnetic field using a commercial 1.8–400 K susceptometer. The magnitude of the ac field was 0.65 mT and the frequency range was 200–1400 Hz . The samples consisted of differing concentrations of dissolved Fe_8 in deionized (DI) H_2O, ~100 μL measured within three hours of mixing in a sealed acrylic sample holder. The χ_{ac} of the holder with DI H_2O was negligible from 1.8 to 3 K.

2.3. NMR relaxometry

The NMR relaxation rates were obtained with a commercial 300 MHz (7 T) NMR system at room temperature within 3 h of mixing. In order to avoid radiation damping (a strong feedback between the transverse magnetization of the aqueous protons and the rf circuit) [22] the Fe_8 and Gd-DTPA (obtained as the commercial preparation Magnevist) were dissolved in a deuterated phosphate buffered saline solution (PBS). The NMR relaxivity r_1 results were obtained by a standard inversion recovery, $\pi_x - \tau - \pi/2_\phi$ – detect, sequence where the protons of the residual water in the sample are initially aligned along the applied field axis z, π_x is a pulse along axis x of such duration and power to invert the spins 180°, τ is a series of times between 0.01 and 2 s varied to obtain the relaxa-

tion along the z-axis, and a $\pi/2_{\phi}$ pulse is used to read out the remaining z-magnetization after the τ delay. A standard cyclically ordered phase sequence (ϕ) is used with the read pulse to eliminate quadrature artifacts. The T_2 relaxation of the H_2O was obtained by the Carr–Purcell–Meiboom–Gill sequence of $\pi_x/2 - (\tau - \pi_y - \tau)_n$ – detect, where multiple echoes were used over the range of 0.01–2 s to measure the spin–spin relaxation in the transverse plane prior to detection of the magnetization. A minimum of eight points were generated for each sequence; these data were processed by the internal NMR software system to generate T_1 and T_2 values for each concentration. The study in Ref. [2] was carried out in an aqueous non-dueterated PBS solution, and that in Ref. [3] in D_2O with the pH adjusted by NaOH.

2.4. MRI

Magnetic resonance images of the contrast agents were obtained with a commercial MRI operating at 64 MHz (1.5 T). Each sample tube was loaded upright in the circularly polarized extremity coil. A series of spin echo sequences were obtained with the following parameters: image matrix 256×256, pixel spacing 0.59 mm × 0.59 mm, slice thickness 5 mm, flip angle 180°, imaging frequency 63.67 MHz, magnetic field strength of 1.5 T, 1 average. The time to repetition (t_r) was 2500 ms and the time to echo (t_e) was varied over a series of 16 images starting at 22 ms and increased at 22 ms increments to 352 ms. A custom program using a simplex algorithm was used to calculate a T_2 map of each sample dilution.

3. Results and discussion

3.1. NMR relaxivity at 300 MHz

The basis of imaging in MRI is the difference in relaxation rates of the imaged aqueous protons due to the local biological environmental. The T_1 weighted image uses fast pulse repetition rates which produce brighter images for shorter T_1 times. T_2 weighted images sample the spin echo at long times weighting protons with long T_2's, which are then brighter. The concept of contrast enhancement using magnetic particles is to selectively shorten either T_1 or T_2 by placing them within proximity of structures of interest, such as lesions and tumors. This is quantified by the relation [23], $(1/T_i)_{obs} = (1/T_i)_d + r_i[M]$ $(i = 1, 2)$, where $(T_i)_{obs}$ is the observed relaxation time of the solvent in the presence of the paramagnetic contrast agent M, and $(T_i)_d$ is the observed relaxation time in the absence of M, and r_i is the relaxivity coefficient that describes the concentration dependence of M. Contrast is generally based on maximizing the difference in relaxation times; therefore a large value of r_i (conventionally in units of $s^{-1}\,mM^{-1}$) indicates large contrast potential. The slope of $(1/T_i)$ as a function of $[M]$ provides r_i.

An examination of the r_i data presented by Refs. [2,3] showed one major difference in the experiments: the concentration range investigated. Here, the relaxivity of Fe_8 is investigated over the entire range of both studies. Fig. 1 shows the inverse T_1 of Magnevist and Fe_8 as a function of concentration over the range of 0.1–3.7 mM. The Magnevist exhibits linear behavior over this range with relaxivity, $r_1 = 5.7\ s^{-1}\,mM^{-1}$, in general agreement with Ref. [3]. On the other hand, Fe_8 exhibited two distinct linear regions, one at low concentration <1.5 mM and one at higher concentrations. The r_1 value at low concentration was $5.4\ s^{-1}\,mM^{-1}$, which compares well to the value of Ref. [2] of $5.1\ s^{-1}\,mM^{-1}$ at 9.4 T. The r_1 value at concentrations above 1.5 mM was $1.1\ s^{-1}\,mM^{-1}$, which compares well with the value reported by Ref. [3] of $1.2\ s^{-1}\,mM^{-1}$, also at 9.4 T. The conflict in the literature is attributed to the concentration range that each group studied.

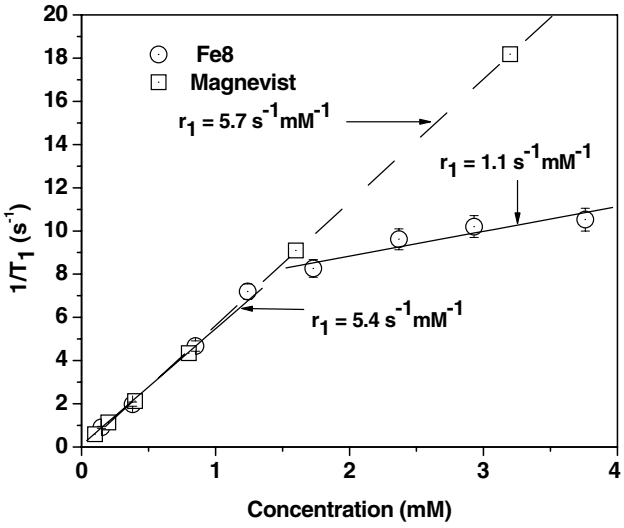

Fig. 1. The inverse proton longitudinal relaxation time T_1^{-1} of 0.1% H_2O in D_2O of Fe_8 and Magnevist solutions as functions of concentration. The Magnevist data are linear across the range investigated. The Fe_8 data, however, show two distinct linear regions above and below 1.5 mM as marked. The slope (r_1) of the low concentration region agrees with Ref. [2], and the slope of the high concentration region agrees with Ref. [3]. These data explain the discrepancy in the literature.

The behavior of T_2^{-1} as a function of contrast agent concentration is shown in Fig. 2. Gd-DTPA (Magnevist) is linear over the entire concentration range with an r_2 of $7.3\ s^{-1}\,mM^{-1}$. In contrast Fe_8 shows two distinct linear regions. Below 1.5 mM the r_2 value is $8.2\ s^{-1}\,mM^{-1}$, compared with Ref. [2] of $8.04\ s^{-1}\,mM^{-1}$. Above 1.5 mM r_2 is $3.2\ s^{-1}\,mM^{-1}$, compared with Ref. [3] of $3.1\ s^{-1}\,mM^{-1}$. Once again, the discrepancy between the two works is attributed to the concentration ranges investigated.

3.2. MRI relaxivity at 64 MHz

The behavior of Fe_8 and Magnevist was investigated using MRI phantoms in DI H_2O at 64 MHz (1.5 T). The MRI signal intensity as a function of the echo time, $S(t_e)$, is related to the transverse relaxation T_2 by [24], $S(t_e) = S_o \exp(-t_e/T_2)$, where S_o is a fit parameter related

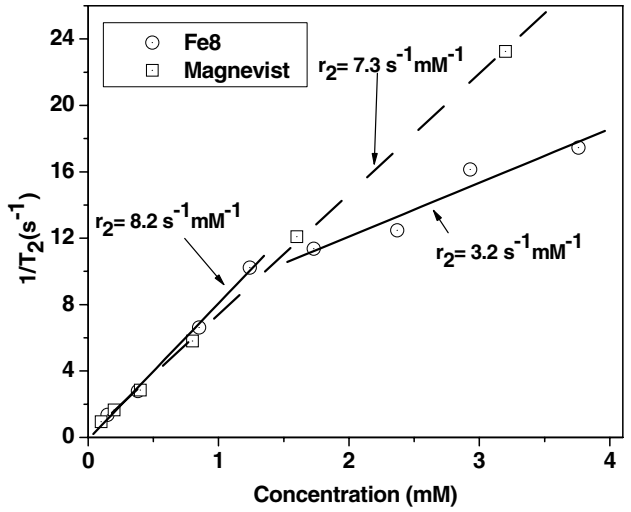

Fig. 2. The inverse transverse relaxation T_2^{-1} of Fe_8 and Magnevist as functions of concentration. In agreement with the relaxation data of Fig. 1, below 1.5 mM the data agree with Ref. [2], and above 1.5 mM the data agree with Ref. [3].

to the initial height of the free induction decay. The values of T_2^{-1} obtained this way as a function of contrast agent concentration are given in Fig. 3. The r_2 for Fe_8 below 1 mM is 4.9 s^{-1} mM^{-1} which compares well with the value in Ref. [2] of 5.01 s^{-1} mM^{-1} obtained by NMR at 1.4 T. Similar to data in Figs. 1 and 2 there is a dramatic decrease in the slope above 1 mM, although more points are needed. This indicates that the concentration dependence of the relaxivity, obtained here by NMR at 300 MHz (7 T), are valid in terms of in vitro MRI at 64 MHz (1.5 T). The relaxivity values are tabulated in Table 1. While the varying conditions and frequencies of these three studies compli-

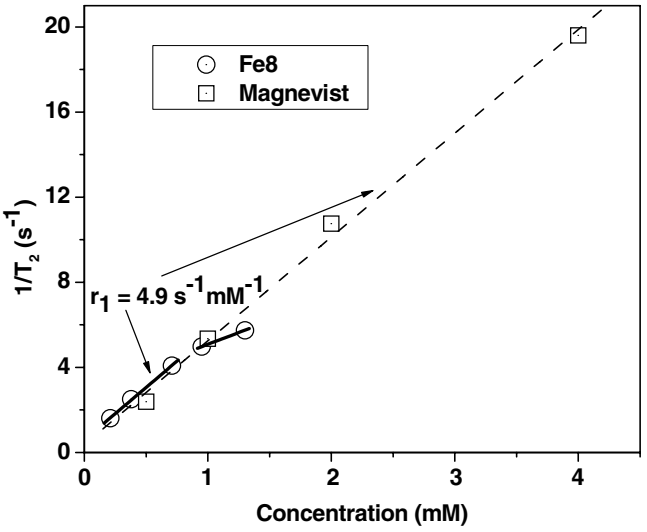

Fig. 3. The inverse transverse relaxation T_2^{-1} of Fe_8 and Magnevist as functions of concentration as obtained from MRI phantoms at 64 MHz (1.5 T). Notice that the $Fe_{8(aq)}$ shows a slope change above 1 mM. This indicates that the data in Figs. 2 and 2 are translatable to clinical in vitro MRI.

Table 1
Comparison of *r*-values

Sample	r_1 (mM^{-1} s^{-1})	r_2 (mM^{-1} s^{-1})	ν (MHz)	Ref.
Fe_8 (<1 mM)	5.10 ± 0.3	8.04 ± 0.12	400	[2]
(<1 mM)	4.76 ± 0.07	5.01 ± 0.08	64	[2]
(<1 mM)		4.9 ± 0.3	64 (MRI)	this work
(<1.5 mM)	5.4 ± 0.3	8.2 ± 0.3	300	this work
(>1 mM)	1.2	3.1	400	[3]
(>1.5 mM)	1.1 ± 0.3	3.2 ± 0.3	300	this work
Gd-DTPA	3.71 ± 0.22	4.44 ± 0.73	400	[2]
	4.29 ± 0.01	4.89 ± 0.02	64	[2]
		4.9 ± 0.3	64 (MRI)	this work
	5.7 ± 0.3	7.3 ± 0.3	300	this work
	5.5	7.0	400	[3]

cate direct *r*-value comparisons, the essential point of concentration dependent *r*-values for Fe_8 seems very clear, and should not depend on the frequency investigated. We are currently evaluating Fe_8 over a wide frequency and temperature range.

3.3. Frozen solution ac susceptibility

In order to assess the degree of stability of the Fe_8 in aqueous solution, we carried out a systematic study of its ac susceptibility using frozen solutions. $Fe_{8(solid)}$ is known to exhibit a frequency-dependent response in the out-of-phase ac susceptibility (χ'') at temperatures of 1.8–5 K [19]. The ac susceptibility of a 6 mM Fe_8 frozen solution was measured by quick insertion into the 1.8 K cryostat of a commercial SQUID magnetometer. In Fig. 4, the dependence of χ''_{ac} as a function of temperature (1.8–3.5 K) and frequency (200–1400 Hz) is shown. A series of maxima which shift to higher temperatures with higher frequencies are present. They are qualitatively similar to the known response of $Fe_{8(solid)}$ observed by Barra et al. [19],

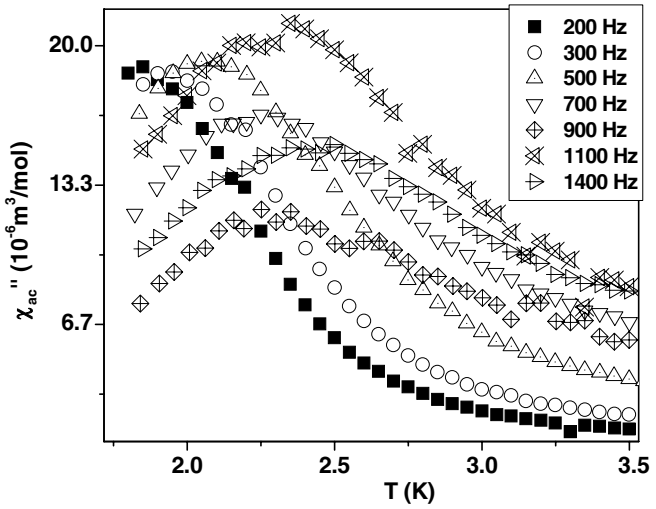

Fig. 4. The χ''_{ac} of a 6 mM frozen solution of Fe_8 in deionized H_2O at an ac field amplitude of 0.65 mT and zero applied dc field. This response is very similar to the response of Fe_8 powder, with the maxima being shifted to lower temperature.

with an overall shift to slightly lower temperature. These data show that in the frozen solution there exists species whose magnetic moment is blocked on the ac time scale at temperatures below 3 K and superparamagnetic above.

The depth of the potential well required to explain the χ'' frozen solution data is of interest for comparison with the Fe_8 solid. For each ac frequency, the temperature of the maxima, T_{max}, in χ'' is inversely related to τ such that at T_{max}, $\tau = (2\pi\upsilon_{ac})^{-1}$. In Fig. 5, the $\ln\tau$ versus the reciprocal of the temperature is plotted and a thermally activated Arrhenius behavior is present. From the slope, $\Delta E/k$ is 14 K and from the intercept $\tau_0 = 3.2\times10^{-7}$ s. The literature values of $\Delta E/k = 24.5$ K and $\tau_0 = 3.4\times10^{-8}$ s have been obtained for $Fe_{8(solid)}$ [18,19]. This approximate agreement suggests the blocked species in Fig. 4 is due to some of the Fe_8 retaining its essential magnetic identity in a frozen solution. The lower value of $\Delta E/k$ with the shift of the maxima to lower temperature implies that the barrier is particle-size and/or conformation dependent: a point that needs additional systematic investigation.

Given the concentration dependence of the relaxivity, the concentration dependence of the χ_{ac} of the Fe_8 frozen solutions was investigated. In Fig. 6. the in-phase response is given, which is sensitive to both blocked as well as paramagnetic species, of the frozen solution at 300 Hz as a function of concentration. At high concentrations, 5 mM for example, a profile characteristic of slow relaxation similar to Fe_8 solid is present, i.e. an inflection point leading to a maximum. This species is then blocked at these time scales and temperatures, and superparamagnetic at temperatures above. At 1 mM, however, a monotonic decrease with increasing temperature is observed indicative of components whose fluctuations are very rapid compared to the observation frequency, such as a paramagnet. The inset shows the molar χ' at 1.8 K as a function of concentration. There is an increase in the χ' as a function of decreasing concentration. Molar susceptibilities should be independent of concentration, this will be discussed later.

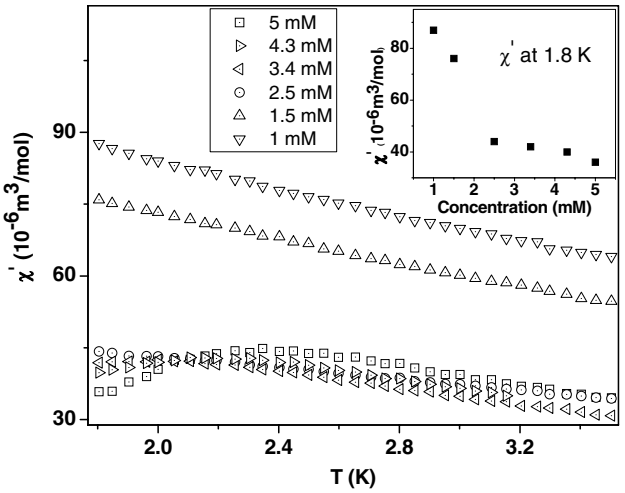

Fig. 6. The concentration dependence of the molar in-phase ac susceptibility at 300 Hz (ac field amplitude of 0.65 mT). The inset shows the χ'_{ac} at 1.8 K as a function of concentration. Note that there is an increase with χ'_{ac} with decreasing concentration.

The out-of-phase susceptibility, which is sensitive only to slow relaxation relative to the observation frequency is given in Fig. 7. At higher concentrations a strong response is observed in the χ'' indicating that the slow relaxation of the magnetic moment is present. As the concentration is lowered below 1.5 mM the maxima in χ'' is much less pronounced. The inset to Fig. 7 shows the maxima in χ'' as a function of concentration. There is a strong increase in the signal at concentrations above 1.5 mM, which roughly corresponds to the break in the $Fe_{8(aq)}$ relaxivity data at room temperature of Figs. 1 and 2.

The data for both low temperature frozen solutions and room temperature relaxivity have demonstrated non-linear

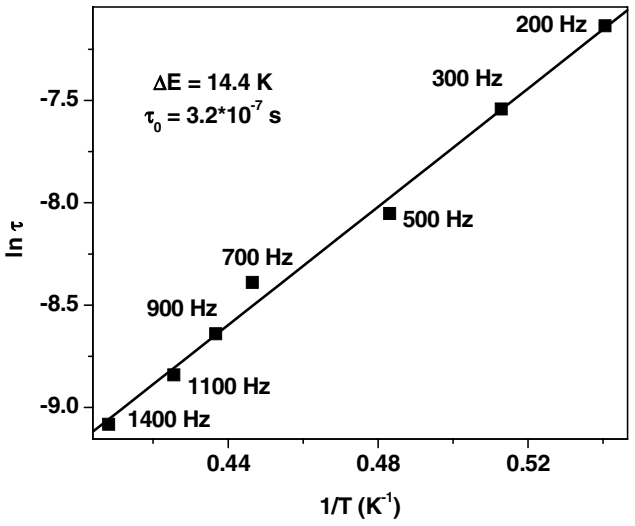

Fig. 5. An Arrhenius plot of the data from Fig. 4 that shows the natural logarithm of the relaxation time as a function of the inverse temperature.

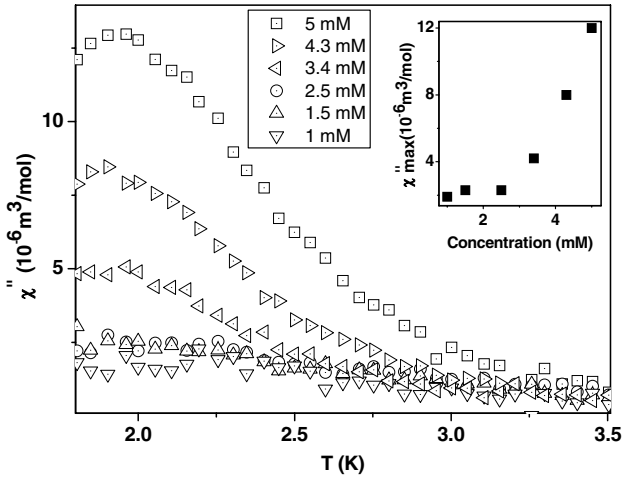

Fig. 7. The concentration dependence of the out-of-phase ac susceptibility at 300 Hz (ac field amplitude of 0.65 mT). Inset shows the maximum as a function of concentration. Notice that there is a non-linear decrease in the molar χ''_{ac} with increasing concentration.

behavior with a break point at ~1.5 mM. In works at concentrations above 1.5 mM both Refs. [3,25] demonstrated that Fe_8 is unstable in aqueous solution. Ref. [3] showed at >1 mM concentrations a partial decomposition into the precursor $Fe(tacn)Cl_3$ occurred. Ref. [25] used Mössbauer spectra of frozen solutions (similar to the conditions in Figs 4 and 5) at concentrations of 5 mM and temperatures of 4 K. Ref. [25] postulated three components; two paramagnetic representing 75% of the spectral area, and a magnetically split (blocked on the Mössbauer time scale) component comprising the remaining 25%. Our high concentration results agree with both works, i.e., that the Fe_8 is unstable in aqueous solutions, and these solutions exhibit blocked superparamagnetic behavior when frozen to low temperatures. However, the data in Fig. 7 show that the molar χ'', which is only sensitive to the blocked superparamagnetic component, seems to decrease at concentrations below 1 mM; while the molar χ' shown in Fig. 6, which is sensitive to the paramagnetic as well as superparamagnetic species, increases as the concentration decreases. In fact, at low concentrations, the molar χ' is essentially paramagnetic in nature.

These results are interpreted as the breakdown of the Fe_8 into small paramagnetic clusters and by-products at low concentrations. As the concentration is increased to around 1.5 mM a saturation of the solution begins to occur. The saturated solution has a much higher degree of relative antiferromagnetic coupling between Fe centers and therefore a lower overall moment per mol or χ'. The species in solution at high concentrations are such, that, when frozen they crystallize out as a compound which has a blocked superparamagnetic component. This component possesses a molar χ'' response similar to Fe_8 powder, but shifted to lower temperatures. This component does not appear to be significantly present at low concentrations.

Does the concentration dependence of the frozen solution data correlate with the room temperature relaxivity? In general, relaxivity scales with moment and sites available for labile water exchange [23]. At concentrations less than 1.5 mM only small paramagnetic Fe clusters or single ions are present. Little antiferromagnetic coupling is present, therefore more moment per mol is available to interact with the aqueous protons. These small clusters and single ions will have more sites available for labile water conjugation directly to the metal centers. At concentrations above 1.5 mM the solution saturates and more Fe–O–Fe interactions come into play. These interactions are antiferromagnetic which reduces the moment per mol as well as the sites available for water exchange, and therefore the relaxivity.

4. Conclusion

We have demonstrated that the discrepancy in the literature regarding the comparative enhancement of relaxation of $Fe_{8(aq)}$ versus the commercial preparation Magnevist is due to the different concentration ranges investigated by each group. Specifically, below 1.5 mM, Fe_8 appears to be competitive with Magnevist, in agreement with Ref. [2], whereas above 1.5 mM it would appear to not compare well with Magnevist, in agreement with Ref. [3]. While the exact nature of the iron particles in the solution phase is unknown, frozen solution χ'' data at concentrations above 1.5 mM strongly suggest that the Fe_8 cores survive in some fashion that contains a magnetically blocked component at low temperatures and superparamagnetic above. Below 1.5 mM the Fe_8 solutions appear to be composed of smaller units that fluctuate magnetically fast on the time scales used in this experiment. The methods here developed of sampling the χ''_{ac} of frozen solutions as a function of frequency and concentration may provide a guideline for future research into the identity and utility of aqueous magnetic species for MRI contrast.

In terms of in vivo utility three factors come to play, toxicity, non-linear relaxivity, and aqueous stability. Ref. [2] pointed out that the concentration normally employed clinically in the extracellular fluid space would be around 0.5 mM. This number is well within the toxicity value of ~1 mM given by Ref. [2]. It is also well within the linear relaxivity range shown in this work of 1 mM or less. While true understanding of the aqueous phase species is desirable, given that the relaxivity at clinical concentrations is comparable to Magnevist, linear, and well within toxicity limits, in vivo experiments would seem to be in order. Further, if the transition from low relaxivity to high relaxivity shown in Figs. 1 and 2 could be taken advantage of, as alluded to in the pH dependence experiments of Ref. [3], perhaps this system could realize a smart contrast mechanism that turns on in the presence of areas of medical interest.

Acknowledgements

We thank Ron Goldfarb of NIST for helpful discussions of aqueous magnetometry and careful reading of the manuscript, and Ruchira Garg of The Department of Pediatric Cardiology, The Childrens Hospital, Denver, CO 80218, for MRI scans, and NSF-DMR (Grant #0506946) for partial support.

References

[1] R.B. Clarkson, Top. Curr. Chem. 221 (2002) 202.
[2] E. Rodriguez, A. Roig, C. Arus, M.R. Quintero, M.E. Cabanas, S. Cerdan, P. Lopez-Larrubia, C. Sanfeliu, NMR Biomed. 18 (2005) 300.
[3] S. Isaacman, R. Kumar, E. del Barco, A.D. Kent, J.W. Canary, A. Jerschow, Polyhedron 24 (2005) 2691.
[4] A. Barker, B. Cage, S. Russek, R. Garg, R. Shandas, C. Stoldt, in: Proceedings of the ASME International Mechanical Engineering Congress and Exposition, Orlando, FL, November 05–11, 2005, IMECE2005-81503.
[5] (a) J.A.A.J. Perenboom, J.S. Brooks, S. Hill, T. Hathaway, N.S. Dalal, Phys. Rev. B 58 (1998) 330;
(b) R. Sessoli, D. Gatteschi, Angew. Chem., Int. Ed. Engl. 42 (2003) 268.

[6] K. Wieghardt, K. Pohl, I. Jibril, G. Hutner, Angew. Chem., Int. Ed. Engl. 23 (1984) 77.
[7] K. Park, M.A. Novotny, N.S. Dalal, S. Hill, P.A. Rikvold, Phys. Rev. B 65 (2002) 014426.
[8] A.L. Barra, D. Gatteschi, R. Sessoli, Chem. Eur. J. 6 (2000) 1608.
[9] D. Zipse, J.M. North, N.S. Dalal, S. Hill, R.S. Edwards, Phys. Rev. B 68 (2003) 184408.
[10] S. Hill, S. Maccagnano, K. Park, R.M. Achey, J.M. North, N.S. Dalal, Phys. Rev. B 65 (2002) 224410.
[11] B. Cage, S.E. Russek, D. Zipse, M. North, N. S Dalal, Appl. Phys. Lett. 87 (2005).
[12] B. Cage, S.E. Russek, D. Zipse, N.S. Dalal, J. Appl. Phys. 97 (2005) 10M507.
[13] S. Maccagnano, R. Achey, E. Negusse, A. Lussier, M.M. Mola, S. Hill, N.S. Dalal, Polyhedron 20 (2001) 1441.
[14] C. Delfs, D. Gatteschi, L. Pardi, R. Sessoli, K. Weighardt, D. Hanke, Inorg. Chem. 32 (1993) 3099.
[15] R. Caciuffo, G. Amoretti, A. Murani, R. Sessoli, A. Caneschi, D. Gatteschi, Phys. Rev. Lett. 81 (1998) 4744.
[16] M.N. Leuenberger, D. Loss, Nature 410 (2001) 789.
[17] W.H. Rippard, M.R. Pufall, S. Kaka, S.E. Russek, T.J. Silva, Phys. Rev. Lett. 92 (2004) 027201.
[18] C. Sangregorio, T. Ohm, C. Paulsen, R. Sessoli, D. Gatteschi, Phys. Rev. Lett. 78 (1997) 4645.
[19] A.L. Barra, P. Debrunner, D. Gatteschi, Ch. E. Schulz, R. Sessoli, Europhys. Lett. 35 (1996) 133.
[20] W. Wernsdorfer, A. Caneschi, R. Sessoli, D. Gatteschi, A. Cornia, V. Villar, C. Paulsen, Phys. Rev. Lett. 84 (2000) 2965.
[21] E. del Barco, J.M. Hernandez, J. Tejada, N. Biskup, R. Achey, N. Dalal, J. Brooks, Phys. Rev. B 62 (2000) 3018.
[22] X. Mao, J. Guo, Ch. Ye, Chem. Phys. Lett. 222 (1994) 417.
[23] R.B. Lauffer, Chem. Rev. 87 (1987) 901.
[24] D.R. McRobbie, E.A. Moore, M.J. Graves, M.R. Prince, MRI: From Picture to Proton, Cambridge University Press, Cambridge, 2004.
[25] E. Rodriguez, M. Gich, A. Roig, E. Molins, N. Nedelko, A. Slawska-Waniewska, A. Szewczyk, Polyhedron 25 (2006) 113.